Open Chem., 2017; 15: 238–246 DE GRUYTER OPEN

Research Article Open Access

Reem I. Al-Wabli, Munusamy Govindarajan, Maha S. Almutairi, Mohamed I. Attia\*

# A combined experimental and theoretical study on vibrational and electronic properties of (5-methoxy-1*H*-indol-1-yl)(5-methoxy-1*H*-indol-2-yl)methanone

https://doi.org/10.1515/chem-2017-0027 received August 23, 2017; accepted October 9, 2017.

9

**Abstract:** (5-Methoxy-1*H*-indol-1-yl)(5-methoxy-1*H*-indol-2-yl)methanone (MIMIM) is a *bis*-indolic derivative that can be used as a precursor to a variety of melatonin receptor ligands. In this work, the energetic and spectroscopic profiles of MIMIM were studied by a combined DFT and experimental approach. The IR, Raman, UV-Vis, <sup>1</sup>H NMR and <sup>13</sup>C NMR spectra were calculated by PBEPBE and B3LYP methods, and compared with experimental ones. Results showed good agreement between theoretical and experimental values. Mulliken population and natural bond orbital analysis were also performed by time-dependent DFT approach to evaluate the electronic properties of the title molecule.

**Keywords:** Indole, Melatoninergic ligand, IR, Raman, DFT, HOMO, LUMO

Reem I. Al-Wabli, Maha S. Almutairi: Department of Pharmaceutical Chemistry, College of Pharmacy, King Saud University, P.O. Box 2457, Rivadh 11451. Saudi Arabia

Munusamy Govindarajan: Department of Physics, Avvaiyar Government College for Women (AGCW), Karaikal, Puducherry 609602, India; Department of Physics, Arignar Anna Government Arts and Science College for Women (AAGASC), Karaikal, Puducherry 609602, India

## 1 Introduction

Indole is the building block of many natural products with diverse biological activities, and hence its derivatives have broad applications in medicinal chemistry [1, 2].

One example is provided by the hormone melatonin (MT), which displays sleep-inducing, antioxidant, anti-inflammatory and antitumor activities. MT contains a 5-methoxyindole core and performs its activity through modulation of G-protein coupling receptors  $MT_1$  and  $MT_2$  [3-5]. Therefore, 5-methoxyindole has been incorporated in a number of melatoninergic ligands [6-8]. (5-Methoxy-1H-indol-1-yl)(5-methoxy-1H-indol-2-l)methanone (MIMIM) is a symmetric bis-5-methoxyindole derivative that can be harnessed as a potential precursor of melatoninergic ligands with improved activity and selectivity.

Density functional theory (DFT) is widely used for the computation of molecular and chemical properties such as geometry, energy and harmonic frequencies [9-11]. Two useful DFT methods are PBEPBE and B3LYP, which furnish sufficiently accurate results for organic compounds at relatively low computational cost. In most cases, both methods provide results that are consistent with experimental ones [12].

The IR, UV-Vis and NMR spectroscopic profiles as well as the electronic properties of MIMIM have not been investigated computationally so far. The aim of this study was to fully determine the energetic and spectroscopic profiles of MIMIM using PBEPBE and B3LYP methods. The results of the current study might assist the design of new melatoninergic ligands bearing 5-methoxyindole moiety.

<sup>\*</sup>Corresponding author: Mohamed I. Attia: Department of Pharmaceutical Chemistry, College of Pharmacy, King Saud University, P.O. Box 2457, Riyadh 11451, Saudi Arabia; Medicinal and Pharmaceutical Chemistry Department, Pharmaceutical and Drug Industries Research Division, National Research Centre (ID: 60014618), El Bohooth Street, Dokki, Giza 12622, Egypt, E-mail: mattia@ksu.edu.sa

# 2 Materials and methods

#### 2.1 General

Melting point was recorded on a Gallenkamp melting point instrument and is uncorrected. The FT-IR spectrum was recorded on a Perkin-Elmer 180 spectrometer in the range of 4000–50 cm<sup>-1</sup>, with a spectral resolution of ±2 cm<sup>-1</sup>. FT-Raman spectrum was recorded using the same instrument equipped with a FRA 106 Raman module (Nd:YAG laser source operating in the region 4000–100 cm<sup>-1</sup> at 1.064 µm line width, 200 mW power). Spectra were recorded with scanning speed of 30 cm<sup>-1</sup>·min<sup>-1</sup> and spectral width of 2 cm<sup>-1</sup>. The frequencies of all sharp bands are accurate to  $\pm 1$  cm<sup>-1</sup>.

## 2.2 Synthesis

A suspension of (5-methoxy-2,3-dihydro-1-H-indol-1-yl) (5-methoxy-1H-indol-2-yl)methanone (0.50 mmol) and 2,3-dichloro-5,6-dicyanobenzo quinone (0.55 mmol) in ethyl acetate (25 mL) was stirred under reflux for 18 h. The reaction mixture was concentrated under reduced pressure and the precipitate collected by filtration. Column chromatography using silica gel and chloroform/ methanol/ammonia (10/1:0/1) as an eluent furnished pure MIMIM (m.p. 178-179 °C) in almost quantitative yield. Spectroscopic data of MIMIM are consistent with those previously reported [13].

#### 2.3 Quantum chemical calculations

Gaussian 03 W program was used to perform the entire quantum chemical calculations at DFT B3LYP and PBEPBE levels with 6-311++G (d,p) basis set [14]. No imaginary frequency modes were obtained at the optimized geometry of the title molecule, so that a true minimum was found on the potential energy surface. As a result, the unscaled calculated frequencies, reduced masses, force constants, infrared intensities, Raman activities and depolarization ratios were obtained. The calculated harmonic frequencies were scaled down to improve the calculated values. Wavenumbers calculated at PBEPBE level were scaled by 0.9067; wavenumbers calculated at B3LYP level were scaled by 0.958 (above 1700 cm<sup>-1</sup>) or by 0.983 (below 1700 cm<sup>-1</sup>) [15, 16]. After scaling, the deviation from experimental values was lower than 10 cm<sup>-1</sup>, with few exceptions. The assignment of calculated normal modes was made based on the corresponding potential energy distributions

(PEDs). PEDs were computed from vibrational frequencies using VEDA program [17]. Gaussview program was used to obtain visual animation and verification of the normal assignment modes [18].

The UV-Vis absorption spectrum of the molecule was calculated by time-dependent DFT (TD-DFT) at PBEPBE/6-311++G (d,p) level of theory. The solvent effect on the UV-Vis absorption spectrum of the molecule was also examined by applying the integral equation formalismpolarized continuum model (IEF-PCM). 1H and 13C NMR chemical shifts of the title compound in CDCl, were calculated using the gauge-independent atomic orbital (GIAO) method. Ethical approval: The conducted research is not related to either human or animals use.

# 3 Results and Discussion

## 3.1 Molecular geometry

Molecular geometry was optimized using PBEPBE method with the atom numbering shown in Figure 1. By allowing the relaxation of all parameters, calculations converged to optimized geometries that correspond to true energy minima, as revealed by the lack of imaginary frequencies in the vibrational mode.

## 3.2 Potential energy scan

Potential energy scan, i.e., the relationship between potential energy and molecular geometry, is a powerful approach to understanding molecular properties. The energy of MIMIM conformers was calculated by the AM1 theory. Two potential energy scans were carried out with the dihedral angles C15-N11-C10-C8 and C18-C17-O23-C24, corresponding to the link of the phenyl ring to the

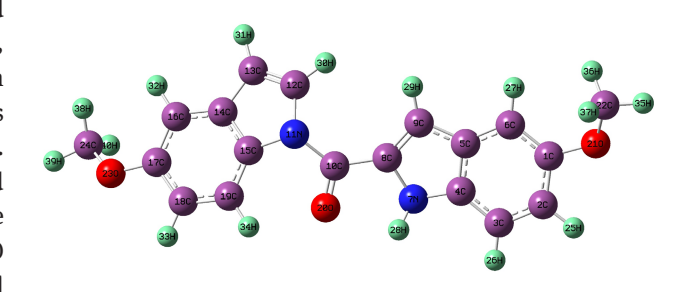


Figure 1: Optimized geometric structure and atom numbering of MIMIM (C<sub>10</sub>H<sub>1</sub>, N<sub>2</sub>O<sub>2</sub>). Atom colors: carbon (violet), hydrogen (green), oxygen (red), nitrogen (blue).

240 — Reem I. Al-Wabli et al.

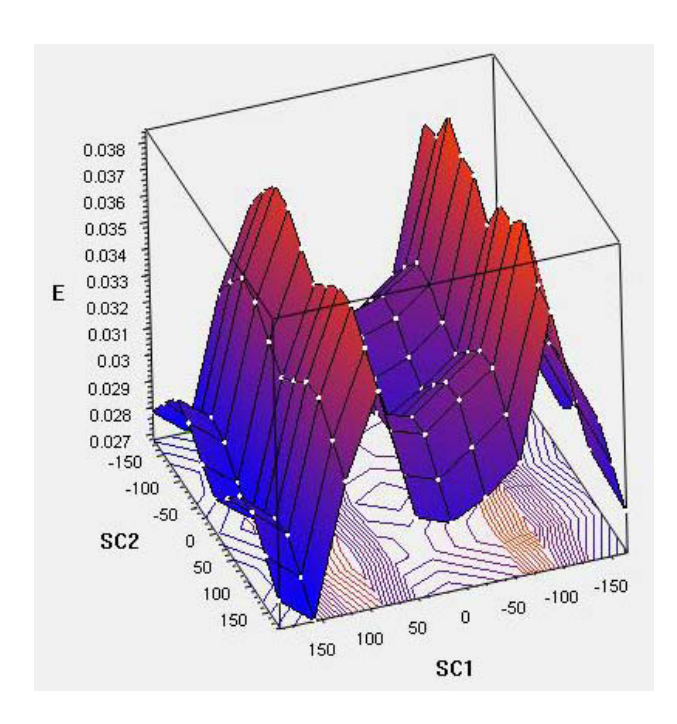


Figure 2: The potential energy scan of the MIMIM molecule.

amide and the methoxy moieties, respectively. During scan, all the geometrical parameters were simultaneously relaxed and varied in steps of 30° from 0 to 360°. The potential energy was calculated for 121 conformers and the curve of potential energy as a function of dihedral angle is shown in Figure 2. Both DFT methods essentially provided the same value of global minimum energy (–1068 a.u. for PBEPBE and –1069 a.u. for B3LYP). The most stable conformer, corresponding to a global minimum energy, has two methoxy groups lying on the same plane.

The optimized bond lengths and bond angles (°) of the most stable conformer were calculated using PBEPBE and B3LYP methods; selected data are listed in Table S1. The optimized geometrical parameters of MIMIM were compared with the experimental values of its crystal structure [19].

The relation between experimental and theoretical values of bond lengths and bond angles of MIMIM are described by the following equations (see Figure S1 for a graphic representation):

$$\begin{split} d_{cal} &= 0.39059 d_{exp.} + 0.3648 & (R^2 = 0.99313) \text{ for bond lengths by PBEPBE method} \\ \delta_{cal.} &= -0.21469 \delta_{exp.} + 1.00311 & (R^2 = 0.96407) \text{ for bond angles by PBEPBE method} \\ d_{cal.} &= 0.73235 d_{exp.} + 0.37812 & (R^2 = 0.99256) \text{ for bond lengths by B3LYP method} \\ \delta_{cal.} &= 1.01124 \delta_{exp.} - 1.20579 & (R^2 = 0.95927) \text{ for bond angles by B3LYP method} \end{split}$$

Good linearity (R<sup>2</sup> >0.99) was observed between calculated and experimental values of bond lengths using both

PBEPBE and B3LYP methods. C–H bond lengths predicted by B3LYP method are systematically too long: average C–H bond length in the MIMIM crystal is 0.96 Å, whereas theoretically calculated values are all >1 Å. The deviation from experimental values may arise from low scattering of hydrogen atoms in the X-ray diffraction experiment. Both B3LYP and PBEPBE methods predict C–N bond lengths in the range of experimental values (1.37–1.41, 1.38–1.41 and 1.36–1.41 Å, respectively). Good agreement is also observed between calculated (B3LYP and PBEPBE) and experimental C–C bond lengths (1.38–1.43, 1.39–1.43 and 1.37–1.42 Å).

Only modest linearity (R<sup>2</sup> >0.95) was obtained between calculated and experimental bond angles. Some experimental values were closer to those calculated by B3LYP method, others were better predicted by PBEPBE method (Table S1). Overall, calculated values showed no significant variation from the experimental ones, except for two bond angles (C3–C4–N7 and C19–C15–N11).

# 3.3 Natural bond orbital analysis

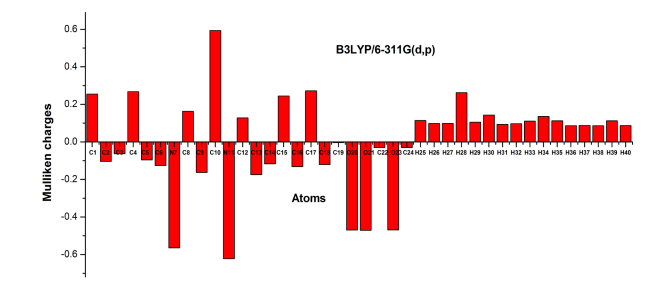
Natural bond orbital analysis was performed to elucidate hyper-conjugation, re-hybridization and delocalization of electron density within the molecule. Analysis highlighted the following intramolecular interactions and energetic contributions: (a) Conjugation of  $\pi(C1-C6)$  to  $\pi^*(C2-C3)$ and  $\pi^*(C4-C5)$  (17.5 and 18.0 kcal/mol, respectively); (b) Hyper-conjugation of  $\sigma(C1-O21)$  to  $\sigma^*(C1-C2)$ , (C1-C6), (C2-C3) and (C5-C6) (1.40, 1.42, 1.44 and 1.42 kcal/mol, respectively); (c) Hyper-conjugation of  $\sigma(C4-N7)$  to  $\sigma^*(C2-V7)$ C3), (C3-C4), (C4-C5), (N7-C8) and (N7-H28) (1.35, 1.34, 1.33, 1.16 and 1.17 kcal/mol, respectively); (d) Delocalization of the lone pair (LP) of N11 to C10-O20 (0.89 kcal/mol); (e) Delocalization of LP of O20 to C8-C10 and C10-N11 (1.10 and 1.02 kcal/mol, respectively); (f) Delocalization of LP of O21 to C1-C2, C1-C6, C22-H35 and C22-H36 (1.08, 1.10, 0.93 and 0.92 kcal/mol, respectively); and (g) LP of 023 to C16-C17, C17-C18 and C24-H38 (1.09, 1.10 and 0.92 kcal/ mol, respectively).

# 3.4 Mulliken charge distribution

Mulliken population analysis was carried out by PBEPBE and B3LYP methods to estimate partial atomic charges of the title molecule (Table 1 and Figure 3). The two methods provided partially contrasting results, as they predict charges of opposite sign on most aromatic carbons. However, according to both methods, most negative charge is localized on the electronegative oxygen and

Table 1: Mulliken charges of MIMIM calculated by PBEPBE and B3LYP methods.

Atom	Method		Atom	Method		
	PBEPBE	B3LYP		PBEPBE	B3LYP	
C1	-0.383015	0.343386	021	-0.277666	-0.523292	
C2	0.377185	-0.126039	C22	-0.239575	-0.074506	
C3	-1.358101	-0.099642	023	-0.279348	-0.522449	
C4	-1.266532	0.326818	C24	-0.234301	-0.073795	
C5	1.199626	-0.043872	H25	0.150876	0.098274	
C6	-0.189779	-0.190254	H26	0.143373	0.091415	
N7	-0.180811	-0.655172	H27	0.135075	0.084764	
C8	-0.026662	0.248235	H28	0.318995	0.276166	
C9	1.184044	-0.181414	H29	0.151492	0.102970	
C10	0.370878	0.553055	H30	0.163488	0.126942	
N11	0.165175	-0.611850	H31	0.145144	0.092249	
C12	-0.507464	-0.095172	H32	0.135309	0.082471	
C13	0.678419	-0.171802	H33	0.149793	0.095022	
C14	-0.032899	0.046603	H34	0.174565	0.125112	
C15	-1.184843	0.283543	H35	0.169858	0.123376	
C16	0.249038	-0.193496	H36	0.165618	0.109501	
C17	-0.053206	0.350608	H37	0.166225	0.110487	
C18	-0.368188	-0.140234	H38	0.164692	0.109097	
C19	0.153927	-0.072157	H39	0.169502	0.122475	
020	-0.464709	-0.514981	H40	0.164802	0.109469	



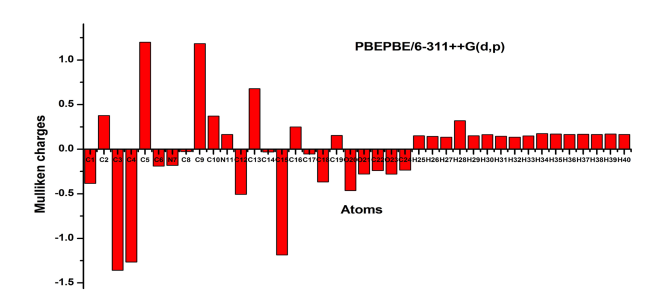


Figure 3. Mulliken charge distribution of MIMIM calculated by B3LYP and PBEPBE methods.

nitrogen atoms; little negative charge is also located on the methoxy carbons as well as the aromatic carbons C12 and C18. Conversely, positive charge is distributed over hydrogen atoms (charge = 0.14-0.17 by PBEPBE method and 0.08-0.28 by B3LYP method).

## 3.5 Frontier molecular orbital analysis

Analysis of frontier molecular orbitals is crucial to understand the physicochemical properties of molecules, because the energy gap between HOMO and LUMO determines the kinetic stability, chemical reactivity, optical polarizability and chemical hardness-softness of the molecule [20][21, 22].

The energy and shape of MIMIM molecular orbitals HOMO-1, HOMO, LUMO and LUMO+1 was calculated using B3LYP method (Table 2 and Figure 4). It is clear from Figure 4 that HOMO is delocalized over almost the whole molecule, whereas LUMO is mainly localized on the rings. The energy difference between HOMO and LUMO in several solvents (acetonitrile, chloroform, cyclohexane, DMSO, ethanol and methanol) varies between 2.55 and 2.60 eV, highlighting a limited solvent effect on molecular energetic profile.

Chemical hardness and electronegativity of MIMIM are 1.27-1.30 eV and 3.64-4.05 eV, respectively.

Dipole moment, being related to the charge distribution within a molecule, determines the intensity of intermolecular interactions, and is therefore an important molecular property. The highest values (>4.0 D) of dipole moment of MIMIM were obtained in highly polar or strong H-bond donor solvents (acetonitrile, DMSO, ethanol and methanol), which are able to stabilize MIMIM charge separation by forming strong intermolecular bonds.

Table 2: Molecular orbital energies calculated for MIMIM.

TD-DFT/B3LYP/ 6-311++G (d,p)	Acetonitrile	Chloroform	Cyclohexane	DMSO	Ethanol	Methanol
E <sub>total</sub> (Hartree)	-1067.518	-1067.515	-1067.511	-1067.518	-1067.582	-1067.518
E <sub>HOMO</sub> (eV)	-5.0361	-4.9954	-4.9339	-5.0377	-5.3243	-5.0353
E <sub>LUMO</sub> (eV)	-2.4491	-2.4003	-2.3469	-2.4513	-2.7704	-2.4483
$\Delta E_{HOMO-LUMO gap}$ (eV)	-2.5869	-2.5950	-2.5869	-2.5863	-2.5538	-2.5869
E <sub>HOMO-1</sub> (eV)	-5.0911	-5.0282	-4.9805	-5.0941	-5.3780	-5.0900
E <sub>LUMO+1</sub> (eV)	-1.3009	-1.2401	-1.1732	-1.3033	-1.6452	-2.3845
$\Delta E_{HOMO-1-LUMO+1 gap}$ (eV)	-3.7902	-3.7880	-3.8073	-3.7907	-3.7327	-2.7055
Electronegativity $\chi$ (eV)	3.7426	3.6978	3.6404	3.7445	4.0473	3.7418
Chemical hardness $\eta$ (eV)	1.2934	1.2975	1.2934	1.2931	1.2769	1.2934
Electrophilicity index $\psi$ (eV )	0.2235	0.2276	0.2297	0.2232	0.2014	0.2235
Dipole moment (Debye)	4.083	3.6961	3.3098	4.0995	4.5116	4.0756

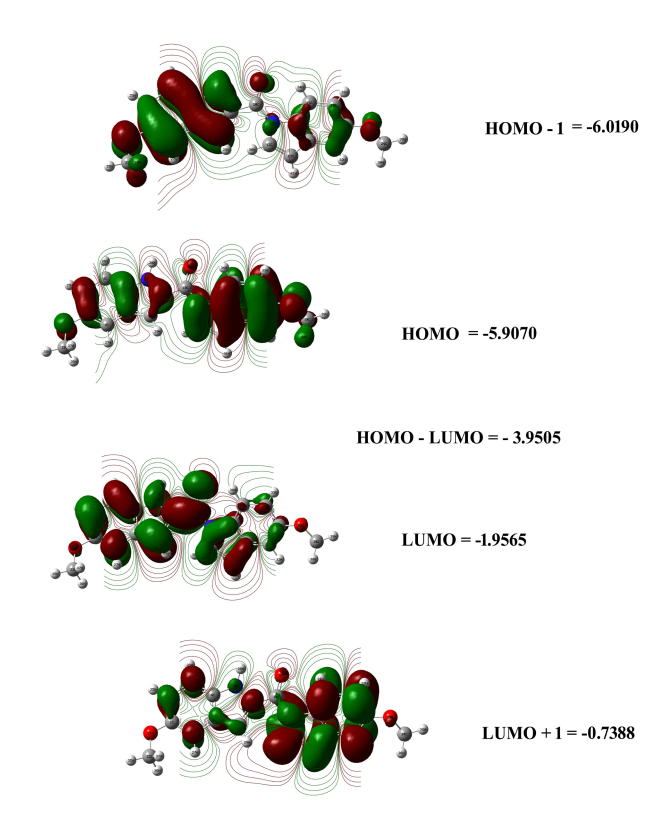


Figure 4: Molecular orbitals and energies of MIMIM (PBEPBE method).

In order to evaluate the energetic behavior of the title compound, we calculated the excitation energies (E), absorption wavelengths ( $\lambda$ ) and oscillator strengths (f) in acetonitrile, chloroform, cyclohexane, DMSO, ethanol and methanol (Table 3). Calculations predicted maximum intensities of electronic transitions at 464, 428, 417, 344 and 327 nm in cyclohexane.

# 3.6 Molecular electrostatic potential and total electron density

The molecular electrostatic potential (MEP) map is a graphic representation of the electrostatic potential of molecules as a function of their constant electron density (ED). MEP illustrates the charge distribution of molecules three-dimensionally in terms of color grading: red < orange < yellow < green < blue. Red color indicates negatively charged areas (with a nucleophilic character), whereas blue color indicates positively charged areas (electrophilic in nature). The negative regions are usually associated with lone pair of electrons on electronegative atoms; positive regions are those having electropositive atoms such as hydrogen atoms. MEP diagram helps understand the relationship between molecular structure and physicochemical properties. MEP and ED of MIMIM are illustrated in Figure 5. The MEP values of MIMIM are in the range of +0.0467 to -0.0467 a.u. The most electronrich – and hence nucleophilic – regions in the molecule correspond to the oxygen atoms of the methoxy and carbonyl groups.

## 3.7 Vibrational analysis

The maximum number of potentially active (i.e., observable) fundamental vibrations of a non-linear molecule containing N atoms is 3N-6, apart from three translational and three rotational degrees of freedom. MIMIM has 40 atoms and therefore 114 normal modes of vibration.

All vibrations are active in Raman and infrared absorptions. The detailed vibrational assignment of

Table 3: Theoretical electronic absorption spectra of MIMIM in various solvents, calculated by TD-DFT/PBEPBE method. Calculated parameters are absorption wavelength  $\lambda$  (nm), excitation energies E (eV) and oscillator strengths (f).

Solvent	E (eV)	λ (nm)	(f)
Acetonitrile	2.7180 eV	456.2 nm	0.0751
	2.8574 eV	433.9 nm	0.0465
	3.0011 eV	413.1 nm	0.1779
	3.5891 eV	345.4 nm	0.3604
	3.7903 eV	327.1 nm	0.0021
Chloroform	2.6936 eV	460.3 nm	0.0759
	2.8732 eV	431.5 nm	0.0607
	2.9860 eV	415.2 nm	0.1668
	3.5895 eV	345.4 nm	0.3759
	3.8178 eV	324.8 nm	0.0049
Cyclohexane	2.6692 eV	464.5 nm	0.0718
	2.8983 eV	428.1 nm	0.0819
	2.9724 eV	417.1 nm	0.1406
	3.6033 eV	344.1 nm	0.3808
	3.7941 eV	326.8 nm	0.0064
DMSO	2.7179 eV	456.2 nm	0.0790
	2.8550 eV	434.3 nm	0.0477
	2.9990 eV	413.4 nm	0.1821
	3.5822 eV	346.1 nm	0.3667
	3.7889 eV	327.2 nm	0.0022
Ethanol	3.4854 eV	355.3 nm	0.0983
	3.5339 eV	350.8 nm	0.0582
	3.6592 eV	338.8 nm	0.4487
	4.0904 eV	303.1 nm	0.2781
	4.3627 eV	284.2 nm	0.0078
Methanol	2.7178 eV	456.2 nm	0.0742
	2.8581 eV	433.8 nm	0.0463
	3.0015 eV	413.1 nm	0.1767
	3.5905 eV	345.3 nm	0.3588
	3.7908 eV	327.0 nm	0.0021

experimental wavenumbers is based on normal mode analysis and comparison with theoretically scaled wavenumbers with PED by B3LYP and PBEPBE methods. Experimental and simulated (PBEPBE method) infrared and Raman spectra of MIMIM are shown in Figures 6 and 7, respectively. Simulations by B3LYP method are reported in Figures S2 and S3. The observed and scaled theoretical frequencies using PBEPBE and B3LYP methods with 6-311++G (d,p) basis set along with their

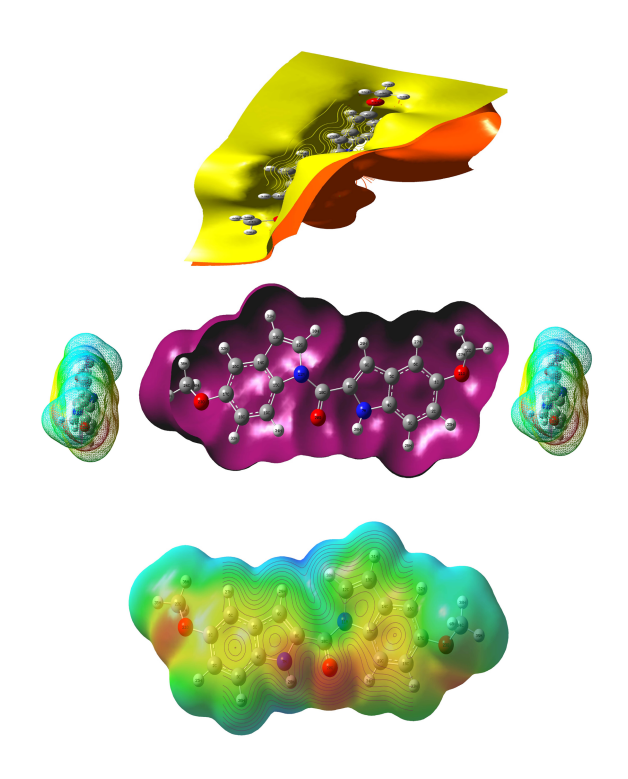


Figure 5: Molecular electrostatic potential (MEP) map and electron density (ED) of MIMIM.

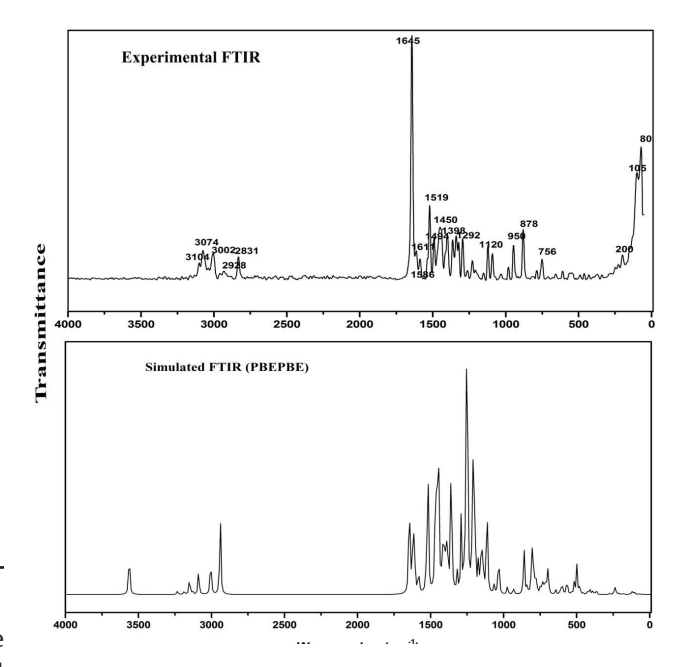


Figure 6: Experimental and simulated (PBEPBE) FT-IR spectra of

PEDs are listed in Table S3. Generally, PBEPBE was more accurate than B3LYP in the prediction of IR and Raman wavenumbers.

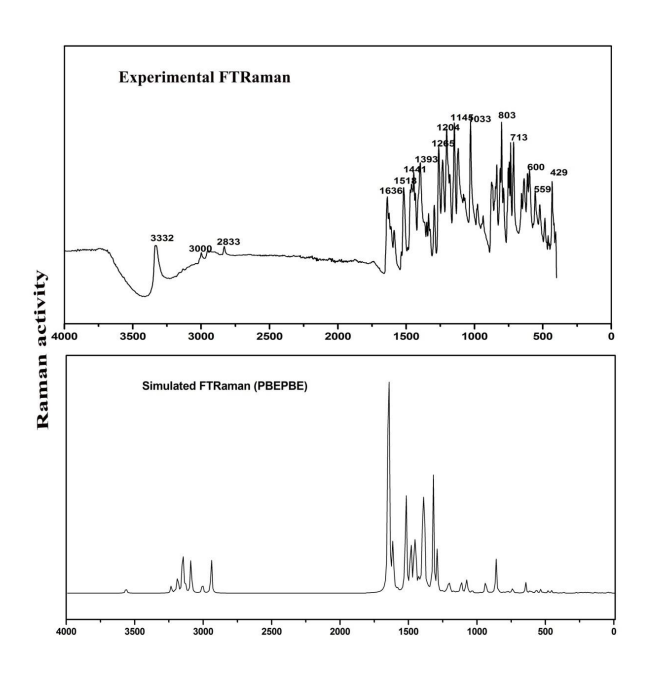


Figure 7: Experimental and simulated (PBEPBE) FR-Raman spectra of MIMIM.

#### 3.7.1 C-H vibrations

MIMIM gave rise to C-H stretching, C-H in-plane and C-H out-of-plane bending vibrations. Aromatic compounds commonly exhibit multiple weak bands in the region of 3100–3000 cm<sup>-1</sup> due to aromatic C–H stretching vibrations which are not appreciably affected by the nature of substituents [22]. MIMIM exhibited one C-H stretching vibration mode at 3074 cm<sup>-1</sup> in its FT-IR spectrum. The symmetric and asymmetric stretching vibrations of the methoxy group generally occur at 2840-2820 and 2970-2920 cm<sup>-1</sup>, respectively [23], whereas asymmetric bending vibrations usually occur at 1460 cm<sup>-1</sup> [24]. The methoxy C-H vibrations of the title compound were observed at 3000 and 2833 cm<sup>-1</sup> in the FT-IR and FT-Raman spectra, respectively, and had either weak or medium intensity. The calculated modes are pure stretching modes, as proved by their 100-91% PED contributions. The measured experimental intensities also support this behavior.

C–H in-plane bending vibrations were observed in the expected region of 1000–1300 cm<sup>-1</sup> [25], specifically at 1265, 1175 and 1146 cm<sup>-1</sup> in the Raman spectrum and at 1155 cm<sup>-1</sup> in the IR spectrum. Most vibrations appeared with very strong intensities.

C–H out-of-plane bending vibrations, which normally appear in the region of 900–675 cm<sup>-1</sup>, were observed at 640, 612 and 419 cm<sup>-1</sup> in the Raman spectrum and identified as pure modes according to PED values.

#### 3.7.2 Ring vibrations

All ring vibrations gave rise to spectral bands of medium or high intensity and were calculated as mixed modes based on their PED contributions.

Aromatic C–C stretching vibrations were observed in the expected range (1400–1600 cm<sup>-1</sup> [26], [27]) at 1606 and 1586 cm<sup>-1</sup> in the IR spectrum and at 1461, 1441, 1435 and 1381 in the Raman spectrum. Calculated values were in excellent agreement with experimental ones.

The infrared band at  $948 \text{ cm}^{-1}$  and the Raman bands at 938, 874, and  $838 \text{ cm}^{-1}$  were assigned to a combination of C–C–C in-plane bending, C–C stretching, and C–H in-plane bending vibrations. The IR bands at  $280 \text{ and } 203 \text{ cm}^{-1}$  were assigned to C–C–C out-of-plane bending vibrations.

#### 3.7.3 C-N vibrations

C–N stretching bands are usually difficult to identify because their position varies considerably depending on the nature of the nitrogen-containing functional group. Significantly different wavenumbers have been observed for the C–N stretching band of aromatic amines (1382–1266 cm<sup>-1</sup>, [28]), pyridines (for instance 1569 and 1469 cm<sup>-1</sup> for 2-formylpyridine, [29]) and indole derivatives (around 1307 cm<sup>-1</sup>, [30, 31]). In the case of MIMIM, IR bands observed at 1365, 1335 and 1265 cm<sup>-1</sup> can be assigned to C–N stretching vibrations based on calculated values (1370, 1336 and 1269 cm<sup>-1</sup>). PED values of these modes suggest they are not pure modes, as it is usually the case for C–N stretching bands.

#### 3.7.4 C=O and C-O vibrations

C=O stretching is one of the strongest IR bands and usually appears in the range of 1680–1640 cm<sup>-1</sup> [32]. MIMIM IR spectrum shows a very strong band at 1636 cm<sup>-1</sup> corresponding to C=O stretching vibration. The C-C=O in-plane bending deformation appears at 1079 cm<sup>-1</sup> in the Raman spectrum with medium intensity, in agreement with the calculated value (1078 cm<sup>-1</sup>, PED = 43%).

C–O stretching vibrations are observed at 1522 and 1486 cm<sup>-1</sup> in the IR spectrum (calculated at 1458 and 1441 cm<sup>-1</sup>, respectively) [33]. The experimental in-plane C–O bending vibration occurred at 803 cm<sup>-1</sup> in the Raman spectrum. The PED values are consistent with the calculated vibrations.

Table 4: Experimental and theoretical <sup>13</sup>C and <sup>1</sup>H NMR chemical shifts of MIMIM in CDCl<sub>2</sub>.

Atom	Experimental	Theoretical PBEPBE/6-311G++ (d,p)	Atom	Experimental	Theoretical PBEPBE/6-311G++ (d,p)
C1	154.90	159.61	H25	7.03	6.73
C2	113.40	112.06	H26	7.37	7.19
C3	109.60	108.30	H27	7.07	6.74
C4	131.60	133.54	H28	9.70	8.49
C5	130.80	131.44	H29	7.08	6.98
C6	102.40	98.40	H30	7.90	7.55
C8	132.50	133.07	H31	6.63	6.43
C9	108.90	108.87	H32	7.09	7.02
C10	160.80	160.92	H33	6.99	6.59
C12	127.60	127.17	H34	8.37	8.24
C13	103.70	99.60	H35	3.85	3.76
C14	129.20	130.69	H36	3.85	3.76
C15	127.80	127.80	H37	3.85	3.76
C16	117.70	118.58	H38	3.87	4.12
C17	156.70	157.65	H39	3.87	4.12
C18	113.00	112.05	H40	3.87	4.12
C19	116.90	116.37			
C22	55.70	55.67			
C24	55.70	55.43			

## 3.8 NMR analysis

<sup>1</sup>H and <sup>13</sup>C NMR chemical shifts of MIMIM were calculated and compared with experimental ones (Table 4). Experimental and theoretical chemical shift values were in good agreement, with a maximum discrepancy of 4.7 ppm for C1 in <sup>13</sup>C NMR spectrum and 1.21 ppm for H28 in <sup>1</sup>H NMR spectrum.

In <sup>1</sup>H NMR spectrum, the most deshielded protons are those belonging to the methoxy groups, due to the electron-withdrawing effect of the oxygen atom. The aromatic ring protons were experimentally observed in the range of 6.99-8.37 ppm, with a substantial overlap to the predicted range (6.59–8.24 ppm).

In <sup>13</sup>C NMR spectrum, aromatic carbons were observed in the expected range (100-160 ppm) in two regions: 102–117 ppm (C2, C3, C6, C16, C18 and C19) and 127–156 ppm (C1, C4, C5, C14, C15 and C17). Aromatic carbons attached to oxygen (C1 and C17) were the most deshielded, whereas carbons adjacent to nitrogen (C4, C8, C12 and C15) were the most shielded.

# **4 Conclusions**

The energetic and spectroscopic profiles of MIMIM were evaluated using PBEPBE and B3LYP methods. The

experimental and simulated IR and Raman spectra are in good fit using the PBEPBE method. The energies of the four molecular orbitals were calculated using the B3LYP method. The molecular electrostatic potential map provided an insight into the electronic molecular properties. MIMIM displayed highest dipole moments in highly polar or H-donor solvents such as acetonitrile or ethanol, respectively. There is a good agreement between the observed and calculated values of 1H and <sup>13</sup>C NMR chemical shifts using PBEPBE method. The characterization of spectroscopic and energetic properties of MIMIM can assist the development of new melatonin receptor ligands with increased potency and selectivity.

Supplementary material: Figures S1-S3 and Tables S1-S3 are provided as supplementary materials.

**Acknowledgments:** The authors would like to extend their sincere appreciation to the Deanship of Scientific Research at King Saud University for its funding of this research through the Research Group Project No. RG-1438-083.

**Conflict of interest:** Authors state no conflict of interest.

# References

- [1] Fu L., Advances in the total syntheses of complex indole natural products. In heterocyclic scaffolds II: Springer, 2010.
- [2] Biswal S., Sahoo U., Sethy S., Kumar H., Banerjee M., Indole: the molecule of diverse biological activities, Asian J. Pharm. Clin. Res., 2012, 5, 1-6.
- [3] Tahan G., Gramignoli R., Marongiu F., Aktolga S., Cetinkaya A., Tahan V., Dorko K., Melatonin expresses powerful antiinflammatory and antioxidant activities resulting in complete improvement of acetic acid-induced colitis in rats, Dig. Dis. Sci., 2011, 56, 715-720.
- [4] Lu J.-J., Fu L., Tang Z., Zhang C., Qin L., Wang J., Yu Z., Shi D., Xiao X., Xie F., Huang W., Deng W., Melatonin inhibits AP-2β/ hTERT, NF-κB/COX-2 and Akt/ERK and activates caspase/Cyto C signaling to enhance the antitumor activity of berberine in lung cancer cells, Oncotarget, 2016, 7, 2985-3001.
- Csernus V., Mess B., Biorhythms and pineal gland. Neuroendocrinol. Lett., 2003, 24, 404-411.
- [6] Attia M.I., Witt-Enderby P.A., Julius J., Synthesis and pharmacological evaluation of pentacyclic 6a, 7-dihydrodiindole and 2, 3-dihydrodiindole derivatives as novel melatoninergic ligands, Bioorg. Med. Chem., 2008, 16, 7654-7661.
- [7] Markl C., Attia M.I., Julius J., Sethi S., Witt-Enderby P.A., Zlotos D.P., Synthesis and pharmacological evaluation of 1,2,3,4tetrahydropyrazino[1,2-a]indole and 2-[(phenyl methylamino) methyl]-1H-indole analogues as novel melatoninergic ligands, Bioorg. Med. Chem., 2009, 17, 4583-4594.
- [8] Markl C., Clafshenkel W.P., Attia M.I., Sethi S., Witt-Enderby P.A., Zlotos D.P., N-Acetyl-5-arylalkoxytryptamine analogs: probing the melatonin receptors for MT<sub>1</sub>-selectivity. Arch. Pharm., 2011, 344, 666-674.
- [9] Nedelec J.M., Hench L.L., Effect of basis set and of electronic correlation on ab initio calculations on silica rings. J. Non-Cryst. Solids, 2000, 277, 106-113.
- [10] Capelle K., A bird's-eye view of density-functional theory, Braz. J. Phy., 2006, 36, 1318-1343.
- [11] Burke K., Perspective on density functional theory, J. Chem. Phy., 2012, 136, 150901.
- [12] Shukla N., Lal A., Vipin V.B., Singh D.K., Comparison of DFT methods for molecular structure and vibrational spectrum of pyrimidine molecule, J. Chem. Pharm. Res., 2014, 6, 59-69.
- [13] Darwish H.W., Attia M.I., New spectrofluorimetric methods for determination of melatonin in the presence of N-{2-[1-({3-[2-(acetylamino)ethyl]-5-methoxy-1H-indol-2-yl}methyl)-5-methoxy-1*H*-indol-3-yl]ethyl}acetamide: a contaminant in commercial melatonin preparations, Chem. Cent. J., 2012, 6,
- [14] Frisch M., Trucks G., Schlegel H.B., Scuseria G., Robb M., Cheeseman J., Montgomery Jr J., Vreven T., Kudin K., Burant J., Gaussian 03, revision C. 02; Gaussian, Inc. Wallingford, CT,
- [15] Arslan H., Algül Ö., Synthesis and ab initio/DFT studies on 2-(4-methoxyphenyl)benzo[d] thiazole, Int. J. Mol. Sci., 2007, 8,760-776.
- [16] Karabacak M., Kurt M., Comparison of experimental and density functional study on the molecular structure, infrared and Raman spectra and vibrational assignments

- of 6-chloronicotinic acid, Spectrochim. Acta A Mol. Biomol. Spectrosc., 2008, 71, 876-883.
- [17] Jamróz M.H., Vibrational energy distribution analysis (VEDA): Scopes and limitations. Spectrochim. Acta A Mol. Biomol. Spectrosc., 2013, 114, 220-230.
- [18] Dennington R., Keith T., Millam J., Eppinnett K., Hovell W.L., Gilliland R., GaussView. Version: 2009.
- [19] Attia M.I., El-Brollosy N.R., El-Emam A.A., Ng S.W., Tiekink E.R., 5-Methoxy-2-[(5-methoxy-1*H*-indol-1-yl)carbonyl]-1*H*-indole, Acta Cryst. E, 2012, 68, o1775-o1775.
- [20] Fleming I., Frontier Orbitals and Organic Chemical Reactions, John Wiley & Sons, USA, 1976.
- [21] Asiri A.M., Karabacak M., Kurt M., Alamry K.A., Synthesis, molecular conformation, vibrational and electronic transition, isometric chemical shift, polarizability and hyperpolarizability analysis of 3-(4-methoxy-phenyl)-2-(4-nitro-phenyl) acrylonitrile: A combined experimental and theoretical analysis, Spectrochim. Acta A Mol. Biomol. Spectrosc., 2011, 82, 444-455.
- [22] Kosar B., Albayrak C., Spectroscopic investigations and quantum chemical computational study of (E)-4-methoxy-2-[(ptolylimino) methyl]phenol, Spectrochim. Acta A Mol. Biomol. Spectrosc., 2011, 78, 160-167.
- [23] Colthup N., Introduction to infrared and Raman spectroscopy, Elsevier, 2012.
- [24] Smith B.C., Infrared spectral interpretation: a systematic approach, CRC Press, USA, 1998.
- [25] Jamróz M.H., Dobrowolski J.C., Brzozowski R., Vibrational modes of 2, 6-, 2, 7-, and 2, 3-diisopropylnaphthalene. A DFT study, J. Mol. Struct., 2006, 787, 172-183.
- [26] Krishnakumar V., Xavier R.J., Normal coordinate analysis of vibrational spectra of 2-methylindoline and 5-hydroxyindane, Indian J. Pure. Appl. Phys., 2003, 41, 95-98.
- [27] Socrates G., Infrared and Raman characteristic group frequencies: tables and charts, John Wiley & Sons, USA, 2004.
- [28] Silverstein R.M., Bassler G.C., Morril T., Spectroscopic identification of organic compounds, John Wiley & Sons, USA,
- [29] Umar Y., Density functional theory calculations of the internal rotations and vibrational spectra of 2-, 3-and 4-formyl pyridine., Spectrochim. Acta A Mol. Biomol. Spectrosc., 2009, 71, 1907-1913.
- [30] Shakila G., Periandy S., Ramalingam S, Molecular structure and vibrational analysis of 3-Ethylpyridine using ab initio HF and density functional theory (B3LYP) calculations, Spectrochim. Acta A Mol. Biomol. Spectrosc., 2011, 78, 732-739.
- [31] Almutairi M.S., Xavier S., Sathish M., Ghabbour H.A., Sebastian S., Periandy S., Al-Wabli R.I., Attia M.I., Spectroscopic (FT-IR, FT-Raman, UV, <sup>1</sup>H and <sup>13</sup>C NMR) profiling and computational studies on methyl 5-methoxy-1H-indole-2-carboxylate: A potential precursor to biologically active molecules, J. Mol. Struct., 2017, 1133, 199-210.
- [32] Silverstein R.M., Webster F.X., Kiemle D.J., Bryce D.L., Spectrometric identification of organic compounds, John Wiley & Sons, USA, 2014.
- [33] Lin-Vien D., Colthup N. B., Fateley W.G., Grasselli J.G., The handbook of infrared and Raman characteristic frequencies of organic molecules, Elsevier, 1991.